Pergamon

Int. J. Heat Mass Transfer. Vol. 39, No. 1, pp. 61–68, 1996

0017-9310/96 $9.50 + 0.00

0017-9310(95)00114-X

Conjugate natural convection in a planar thermosyphon with multiple inlets—II. Heat transfer

JOHN FLEMING and M. RUHUL AMIN†

Department of Mechanical Engineering, Montana State University, Bozeman, MT 59717, U.S.A.

(*Received* 18 *May* 1994 *and in final form* 24 *February* 1995)

Abstract—The heat transfer results for the numerical investigation of a planar open loop thermosyphon with conducting walls are presented. Laminar natural convection is due to heating the left ascending channel of a modified 'U' type thermosyphon with an upper and lower inlet in the right descending channel. Governing parameters investigated include the Rayleigh number (Ra), the ascending channel aspect ratio (Ar) and the lower inlet width (W_2). Another parameter which combines the heated wall geometry and thermal conductivity is demonstrated to correlate the heat transfer results well. The average non-dimensional heat flux (Φ) is strongly affected by the wall thermal conductivity, primarily due to conduction resistance of the heated wall. For restrictive W_2 and low Ra, Φ decreases. At large Ra, however, Φ depends little on W_2. This is due to compensating inflow at the outlet (recirculation).

1. INTRODUCTION

The primary purpose of this study is to investigate the heat transfer characteristics of a planar open loop thermosyphon with conducting walls and multiple flow inlets. A detailed description of the fluid flow and temperature fields for the thermosyphon configuration of interest is presented in Part I [1]. For brevity and completeness of this paper, only a diagram of the problem geometry with pertinent nomenclature is shown in Fig. 1.

Few studies of natural convection heat transfer in channels have explicitly taken into account the thickness and finite thermal conductivity of the bounding wall surfaces. Zinnes [2] studied numerically the wall conduction effects for laminar natural convection from a single vertical wall with arbitrary heating. He found that the wall to fluid thermal conductivity ratio (k_w/k_a) was a useful parameter for correlation of the heat transfer results. Other research [3–5] also indicated that conducting wall effects are often significant with respect to heat transfer and should not be neglected in many instances.

Another parameter that characterizes wall conductivity was presented by Kaminski and Prakash [6] who studied the effects of wall conduction in a square enclosure. They investigated numerically the overall heat transfer effects as a function of several parameters, namely: Grashof and Prandtl numbers, wall thickness to height ratio (h_1/l_1), and wall to fluid thermal conductivity ratio (k_w/k_a). Their results indicated that for a constant value of $k_w l_1/k_a h_1$ the overall heat transfer was independent of k_w/k_a and l_1/h_1 separately. The enclosure fluid 'sees' the same thermal driving force, and thus the overall heat transfer was correlated well with this parameter.

The heat transfer effects due to a modification of the typical 'U' open loop flow path is also of interest here. An additional lower inlet at the base of the right

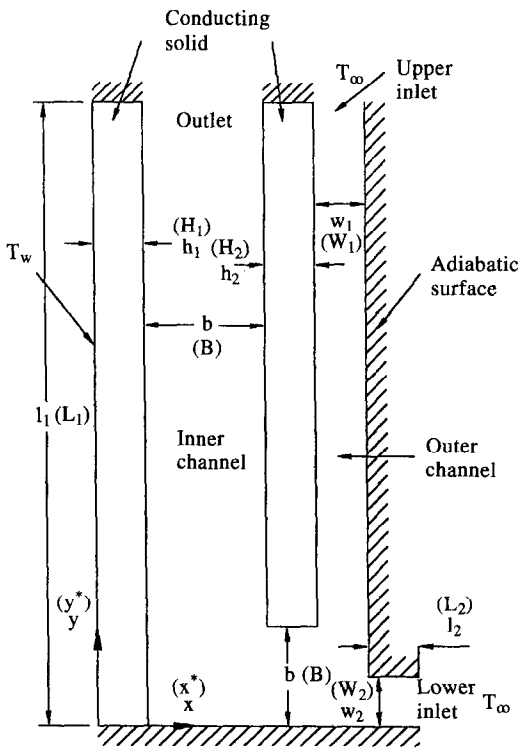

Fig. 1. Schematic diagram of problem geometry.

† Author to whom correspondence should be addressed.

NOMENCLATURE

Ar	inner channel aspect ratio, l_1/b
b	dimensional inner channel width
B	non-dimensional inner channel width, b/b
g_y	acceleration due to gravity
h_1	dimensional left wall thickness
H_1	non-dimensional left wall thickness, h_1/b
k	thermal conductivity
K	thermal conductivity ratio, k_w/k_a
K_r	wall conductivity parameter, $K_r = (k_w/k_a)(l_1/h_1)$
l_1	dimensional inner channel height
L_2	non-dimensional lower inlet length, l_2/b
Nu	average Nusselt number, $(l_1/k_a)\bar{q}/(T_i - T_\infty)$
p_m	motion pressure
Pr	Prandtl number, ν/α
$\bar{q}$	average heat flux at hot wall
Ra	Rayleigh number, $g_y\beta\,(T_w - T_\infty)b^3/\alpha\nu$
T	temperature
u	velocity
u_{max}	maximum velocity
$\mathbf{u}$	velocity vector
U_0	characteristic velocity
W_1	non-dimensional upper inlet width, w_1/b
W_2	nondimensional lower inlet width, w_2/b
x	Cartesian x coordinate
y	Cartesian y coordinate.

Greek symbols

α	thermal diffusivity
β	coefficient of volumetric expansion
θ	non-dimensional temperature $(T - T_\infty)/(T_w - T_\infty)$
ν	kinematic viscosity
ρ	density
Φ	average non-dimensional heat flux, $(b/k_a)\bar{q}/(T_w - T_\infty)$.

Subscripts

a	working fluid (air) value
i	solid-to-fluid interface value
l	published value
p	partition wall value
w	heated wall value
∞	ambient value.

Superscript

*	non-dimensional quantity.

flow channel augments the inflow from the upper inlet. It has been shown previously [1] that the lower inlet affects the thermosyphon flow and temperature fields. This article extends the investigation to the effects on the overall heat transfer.

2. ANALYSIS

The function of the previous non-dimensional formulation [1] was primarily to isolate relevant non-dimensional parameters. All numerical solutions were performed using the primitive variables as required by the proprietary finite element program [7] utilized here and discussed previously [1]. Thus, the normalized governing equations and boundary conditions are not used here for numerical computations. The non-dimensional independent and dependent variables are restated below:

$$x^* = \frac{x}{b} \quad y^* = \frac{y}{b} \tag{1}$$

$$\mathbf{u}^* = \frac{\mathbf{u}}{U_0} \quad \theta = \frac{(T - T_\infty)}{(T_w - T_\infty)} \quad p_m^* = \frac{p_m}{\rho U_0^2}. \tag{2}$$

Relevant non-dimensional parameters arise through the normalization of the dependent and independent variables and subsequent normalization of the governing equations and boundary conditions. Thus, the method used to normalize the dependent and independent variables is critical so that important parameters are not overlooked.

The dimensionless variables shown in equations (1) and (2) require some explanation, particularly concerning the characteristic velocity U_0. There is no obvious velocity scale (characteristic velocity) for buoyancy-driven flows, but U_0 may be estimated. One estimation method [8] equates the kinetic energy per unit volume of the flow, $\rho u^2/2$, to the work done per unit volume by the buoyancy force, $-g_y(\rho - \rho_\infty)$, over some characteristic length (l_1). This is shown below:

$$\rho\frac{u^2}{2} = -g_y(\rho - \rho_\infty)l_1 = \rho g_y\beta(T_w - T_\infty)l_1. \tag{3}$$

Solving equation (3) above for velocity u, and keeping in mind the definitions for Ra and Ar, the characteristic velocity is found:

$$u_{max} = U_0 = \sqrt{[g_y\beta(T_w - T_\infty)l_1]} = \frac{\alpha}{b}\sqrt{Ra\,Pr\,Ar} \tag{4}$$

where

$$Ra = \frac{g_y\beta(T_w - T_\infty)b^3}{\alpha\nu} \quad Pr = \frac{\nu}{\alpha} \quad Ar = \frac{l_1}{b}. \tag{5}$$

The characteristic velocity (U_0) defined above has been used previously [1] to normalize the governing equations; however, a more realistic estimation is possible. The development of this estimate is the subject of the following paragraphs. First, it should be made clear that the objective here is to show the existence and theoretical basis for another non-dimensional parameter not previously apparent.

The problem with the definition for U_0 [equation (4)] is the temperature difference $(T_w - T_\infty)$; the actual temperature difference across the fluid is $(T_i - T_\infty)$, where T_i is the temperature of the fluid-to-solid interface along the heated wall. Due to low wall thermal conductivity, T_i may be considerably less than T_w. Thus, U_0 depends more realistically on $(T_i - T_\infty)$ rather than $(T_w - T_\infty)$.

A better estimate for U_0 is found by estimating the temperature difference $(T_i - T_\infty)$. Assuming one-dimensional heat conduction across the heated wall, $(T_i - T_\infty)$ is estimated in equation (6) below. The parameter K_r which appears below is the product of the thermal conductivity ratio (K) and the heated wall aspect ratio (l_1/h_1), and is expressed by equation (7). This result [equation (6)] is substituted into equation (4) with the resulting U_0 shown in equation (8).

$$(T_i - T_\infty) \approx \frac{K_r}{K_r + Nu}(T_w - T_\infty) \tag{6}$$

$$K_r = \left(\frac{k_w}{K_a}\right)\left(\frac{l_1}{h_1}\right) = K\left(\frac{l_1}{h_1}\right) \tag{7}$$

$$U_0 = \frac{\alpha}{b}\left(Ra\,Pr\,Ar\left(\frac{K_r}{Nu + K_r}\right)\right)^{1/2}. \tag{8}$$

Here the average Nusselt number (Nu) is computed by averaging the local heat flux over the surface of the heated wall. This is shown in equation (9) using the fluid thermal conductivity (k_a), the solid-to-fluid interface temperature difference, the heated wall length (l_1), and the average wall heat flux ($\bar{q}$). Note that this definition is relevant only for this discussion and is not used to present results of this study. The equation used to present the heat transfer results is introduced later by equation (14)

$$Nu = \frac{\bar{q}}{T_i - T_\infty}\frac{l_1}{k_a}. \tag{9}$$

The parameter K_r is the same as that presented by Kaminski and Prakash [6]. Essentially, this shows the dependence of the characteristic velocity U_0 on the parameter K_r and illustrates that a more physically accurate scaling of the governing equations should include this parameter. This is shown explicitly in equations (10)–(13), namely: the continuity, the momentum, and the energy equations for the fluid region and the solid regions. Results of this study are used to verify that K_r is a useful parameter for correlation of overall heat transfer results

$$\nabla \cdot \mathbf{u}^* = 0 \tag{10}$$

$$(\mathbf{u}^* \cdot \nabla)\mathbf{u}^* = -\nabla p_m^* + \sqrt{\left[\frac{Pr(Nu + K_r)}{Ra\,Ar\,K_r}\right]}\nabla^2 \mathbf{u}^* + \theta\frac{(Nu + K_r)}{Ar\,K_r} \tag{11}$$

$$(\mathbf{u}^* \cdot \nabla\theta) = \nabla^2\theta\sqrt{\left[\frac{Nu + K_r}{Ra\,Pr\,Ar\,K_r}\right]} \tag{12}$$

$$\nabla^2\theta = 0. \tag{13}$$

It should be noted that the above non-dimensional equations are developed here to identify the important non-dimensional parameters which affect the heat transfer rate of the present thermosyphon. As discussed earlier, the governing equations were solved in terms of the primitive variables.

3. NUMERICAL INVESTIGATION

Consideration of the above normalized governing equations indicates that a parametric study of the heat transfer characteristics involves the non-dimensional parameters Ra, Ar, Pr, Nu and K_r. One other geometric parameter of interest which does not appear explicitly in the normalized governing equations but appears in the boundary conditions is the lower inlet width W_2.

For this study $Pr = 0.71$ was used, representing air as the working fluid. To limit further the study Ar was held constant, and the overall heat transfer rate, equation (14), was investigated rather than the non-dimensional average convection coefficient Nu. To examine the effects of the remaining parameters (Ra, K_r, W_2) on the heat transfer rate, each was varied independently of the others over the range of interest. In this study, the ranges of Ra, K_r and W_2 were chosen to be 10^3–10^6, 1.2–120 and 0.0–0.75, respectively. A detailed computational matrix in this regard is listed by Fleming [9].

As described in Part I [1], the governing equations were solved numerically for a total of 128 cases corresponding to the parameter values. The heat transfer results are presented here using the wall conductivity parameter (K_r) rather than the thermal conductivity ratio (K). Use of the parameter K_r may be advantageous in a parametric study of wall conductivity effects. This is because it essentially lumps two parameters, namely a geometric parameter and a thermophysical parameter, into one parameter. A study of the parameter K_r was conducted here to ensure that it adequately characterizes the heated wall.

4. RESULTS AND DISCUSSION

4.1. *Wall conductivity parameter*

To study the effects of K_r, the overall heat transfer rate is compared for cases where K_r is a constant, but the wall geometry and thermal conductivity vary.

Table 1. Wall conductivity study parameters with $Ar = 6$ and $W_2 = 0.5$

Case number	l_1/h_1	$K = k_w/k_a$	K_r
1	60	1	60
2	12	5	60
3	24	5	120
4	12	10	120

Table 1 shows the cases considered. Recall that the partition wall has the same thermal conductivity as the heated wall. Thus, cases 1 and 2 or 3 and 4 should not be compared directly unless it is shown that changing the thermal conductivity of the partition wall has negligible effect on the overall heat transfer rate.

The conducting partition wall complicates the heat transfer by introducing temperature-dependent flow conditions at the upper inlet channel. If the partition wall were adiabatic, flow inside the upper inlet channel would approach isothermal flow due to pressure gradients only. With a conducting partition, however, thermal buoyancy forces oppose the flow.

Buoyancy forces at the upper inlet are due to heat energy transferred across the partition originating at the left heated wall. Heat transfer from the heated wall to the partition (across the inner channel) is by conduction in the fluid region because there is no fluid velocity in this direction. Thus, flow restriction due to the partition heat transfer is expected to decrease with increasing Ra (decreased conduction effects).

To study the effect of partition conduction, the total heat transfer through the partition (Φ_p) as a percentage of total heat transfer at the heated wall (Φ) is shown as a function of Ra and K_r in Fig. 2. The total heat transfer through the partition was computed by integration of the computed temperature gradients at the nodes along the partition right surface.

Recall from equation (7) that K_r is the product of the conductivity ratio (k_w/k_a) and the heated wall aspect ratio (l_1/h_1). The results of Fig. 2 are presented for $l_1/h_1 = 12$. Therefore, any change in the value of K_r in this case actually represents the change in the wall thermal conductivity k_w. The other parameters, k_a, l_1/h_1 and Ar are constant in Fig. 2.

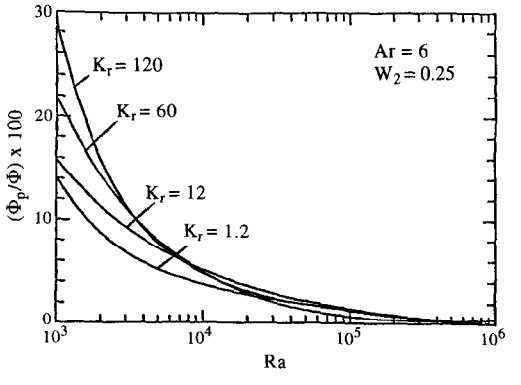

Fig. 2. Heat transfer to upper inlet as a percentage of total heat transfer.

From the figure it can be seen that increasing K_r does increase the partition heat transfer, but only at relatively low Ra ($\leqslant 2 \times 10^4$). For larger Ra, conduction across the inner channel is so reduced that the partition thermal conductivity is irrelevant. This indicates that flow restriction due to opposing buoyancy forces is only relevant at low Ra. Thus, cases 1 and 2 or cases 3 and 4 (of Table 1) may be compared directly for Rayleigh numbers greater than 2×10^4.

The overall heat transfer (Φ) for the hot wall is calculated using equation (14). It is customary to refer to Φ as a non-dimensional average heat flux. Note that since Φ is evaluated on the basis of $(T_w - T_\infty)$, it is more appropriate to interpret Φ as the non-dimensional heat flux rather than the non-dimensional convective heat transfer coefficient:

$$\Phi = \frac{\bar{q}b}{k_a(T_w - T_\infty)} = \frac{k_w}{k_a}\frac{b}{l_1}\frac{1}{(T_w - T_\infty)}\int_0^{l_1}\frac{\partial T}{\partial x}\mathrm{d}y. \tag{14}$$

The non-dimensional average heat flux results for cases 1–4 are given in Table 2. It is clear that for constant K_r, Φ changes only slightly even though wall geometry and thermal conductivity are dramatically different. The maximum percentage difference in this study is found to be 0.22, thus K_r appears to be an independent parameter in this study. Therefore, it is established that for fixed values of Ra and K_r, the overall heat transfer rate does not change even though the heated wall aspect ratio and thermal conductivity have changed. This is a very important observation and is in agreement with the findings of Kaminski and Prakash [6].

A comparison of Φ for Rayleigh numbers less than 2×10^4 is shown in Table 3. This comparison provides a quantitative criterion for gauging how important opposing buoyancy effects in the upper inlet channel are with respect to overall heat transfer. Table 3 indicates that overall heat transfer is affected very little. The maximum percentage difference in Φ for these cases is found to be 0.46. This is observed at the lowest value of Ra (10^3), therefore it can be concluded that even at lower values of Rayleigh number, the overall heat transfer rate is affected very little for a fixed value of K_r. Note that this does not mean that flow in the upper inlet is not affected by changing the partition thermal conductivity. It is shown in ref. [1] that the flow in the upper inlet does change with changes in partition thermal conductivity. It will also be shown in the following section that the overall heat transfer rate changes with changing wall thermal conductivity.

These results indicate that the parameter K_r correlates the overall heat transfer and agrees well with the findings of ref. [6]. However, it is expected that the temperature field will vary locally for cases with constant K_r. Consider cases 1 and 2 of Table 1; increasing the wall conductivity K should tend to

Table 2. Overall heat transfer results for K_r study ($Ra > 2 \times 10^4$)

	Average non-dimensional heat flux (Φ)					
Ra	Case 1 $K_r = 60$	Case 2 $K_r = 60$	% Difference	Case 3 $K_r = 120$	Case 4 $K_r = 120$	% Difference
5×10^4	3.322	3.319	0.09	4.075	4.070	0.12
10^5	3.647	3.640	0.19	4.571	4.565	0.13
2.5×10^5	4.109	4.100	0.22	5.319	5.312	0.13
5×10^5	4.475	4.468	0.16	5.947	5.943	0.07
10^6	4.846	4.840	0.12	6.615	6.610	0.08

Table 3. Overall heat transfer results for K_r study ($Ra < 2 \times 10^4$)

	Average non-dimensional heat flux (Φ)					
Ra	Case 1 $K_r = 60$	Case 2 $K_r = 60$	% Difference	Case 3 $K_r = 120$	Case 4 $K_r = 120$	% Difference
10^3	1.531	1.524	0.46	1.681	1.676	0.30
5×10^3	2.297	2.299	0.09	2.662	2.658	0.15
10^4	2.617	2.622	0.19	3.089	3.087	0.06

make the solid-to-fluid interface temperature distribution more uniform. Larger K facilitates conduction in the vertical direction which tends to equalize local temperature fluctuations. In Fig. 3 the heated wall solid-to-fluid interface temperature distribution (θ_i) is plotted. It shows that for a fixed value of K_r, increasing the value of K does reduce the local temperature fluctuations. Here the value of K_r is kept constant with changing K, by changing the wall aspect ratio (l_1/h_1).

4.2. *Overall heat transfer dependencies*

As mentioned earlier, the overall heat transfer rate is represented by the average non-dimensional heat flux Φ, and is expressed by equation (14). Figures 4 and 5 show the dependence of Φ on the parameters Ra, W_2 and K_r. It can be seen from the fixed K_r plots of Fig. 4 that Φ increases with increasing Ra and W_2. However, for sufficiently large Rayleigh numbers

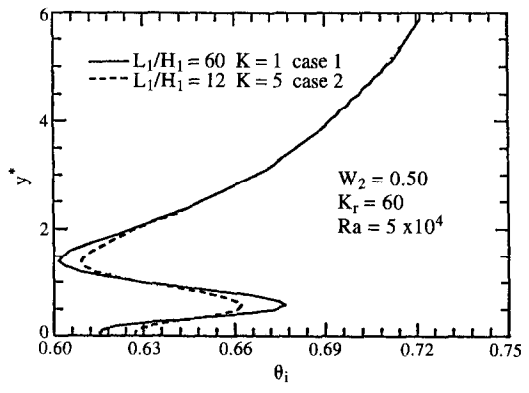

Fig. 3. Constant K_r solid-to-fluid interface temperature distribution comparison, cases 1 and 2.

($> 10^5$), Φ becomes nearly independent of W_2. At lower Rayleigh numbers, Φ depends on both W_2 and K_r. For values less than 0.5, W_2 strongly affects Φ. Increasing W_2 beyond 0.5 has little impact on Φ ($< 2\%$). It is evident that the effects of W_2 tend to diminish with larger K_r. Once again, note that in these cases (l_1/h_1) and Pr are kept constant. Thus, any change in K_r actually represents the change in wall thermal conductivity k_w.

Examination of Fig. 5 reveals that Φ tends to increase dramatically with K_r. The heat transfer enhancement due to the effects of K_r appears stronger at higher values of Rayleigh number. It is evident that Φ depends on K_r over the full range of Rayleigh numbers investigated. In all the cases investigated in this research, improved heat transfer is achieved with increasing K_r and/or W_2.

A few comments regarding the parameters K_r and W_2 will aid the interpretation of the trends described above. Note that for cases with fixed aspect ratio, Ar, and fixed K_r (Fig. 4), flow restrictions and Ra possess the only potential for affecting Φ. The partition wall and other boundaries cause flow restrictions that are not adequately represented by W_2. These flow restrictions essentially limit the physical access of the cool reservoir fluid to the heated wall and are inherent in the thermosyphon geometry.

As noted previously, for Rayleigh numbers greater than 10^5, Φ is almost independent of W_2. With respect to Fig. 5, this indicates that at large Rayleigh numbers ($> 10^5$) any change in Φ is due to changes in the parameters K_r, Ra and any flow restrictions not represented by W_2. Keeping in mind the points discussed above, the trends of Figs. 4 and 5 are next examined to determine causes for the observed behavior.

In Part I [1] in which effects due to W_2 were studied,

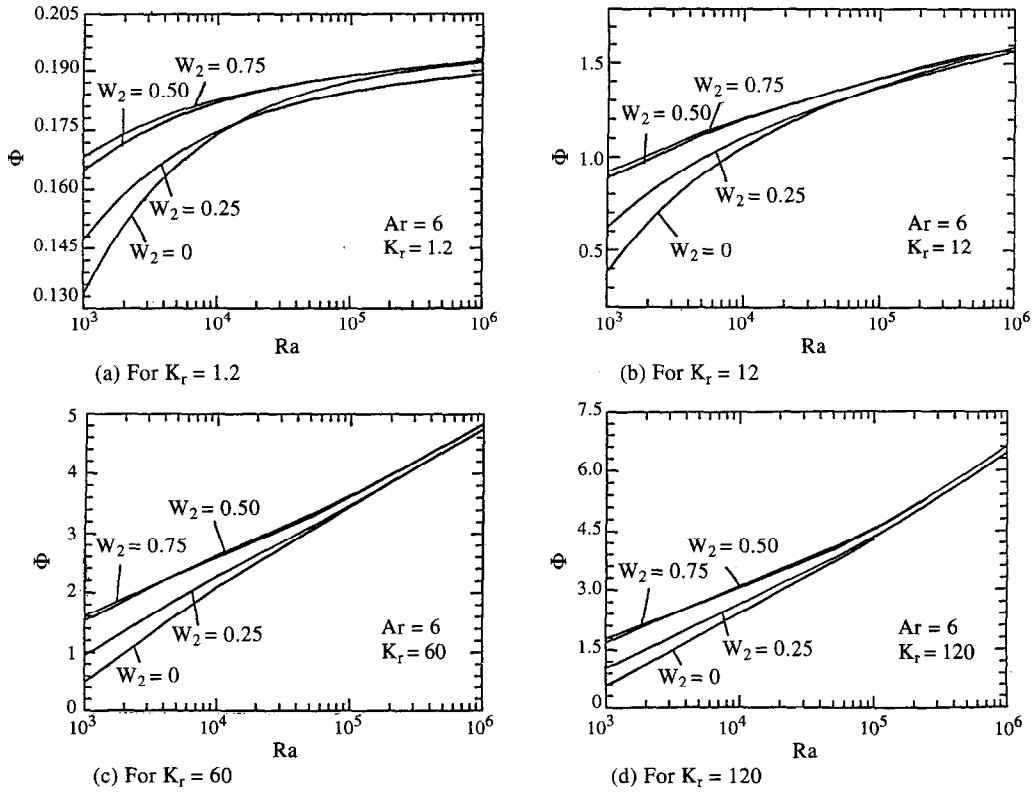

Fig. 4. Average non-dimensional heat flux (Φ) vs Rayleigh number with parameters W_2 and K.

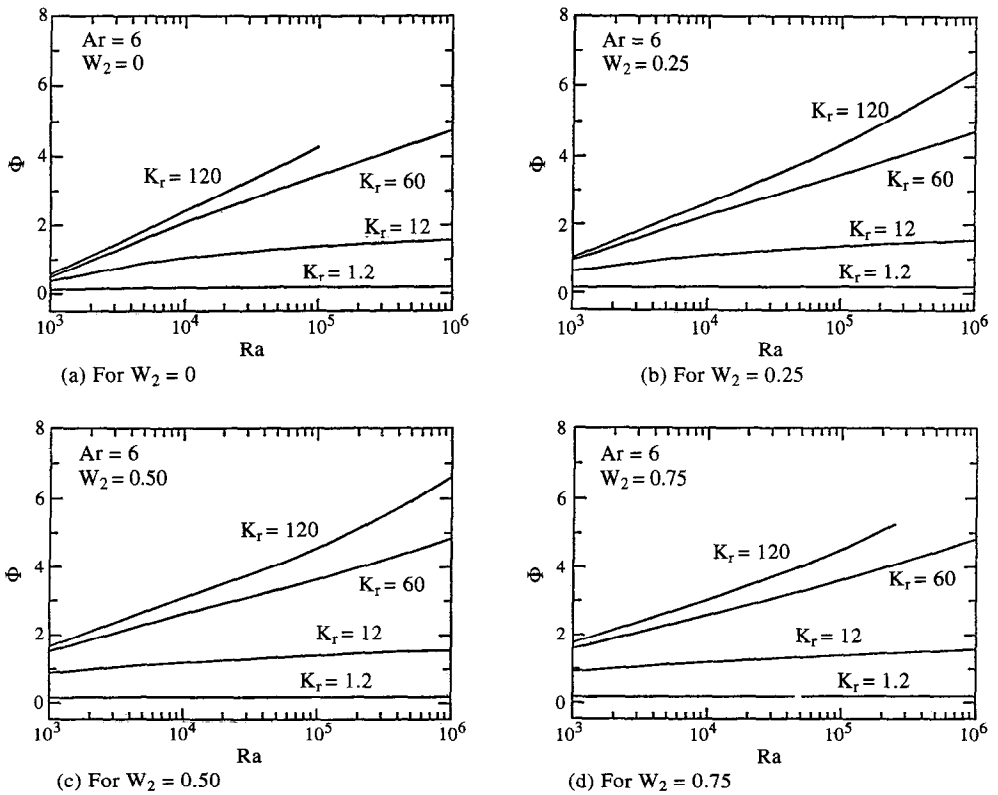

Fig. 5. Average non-dimensional heat flux (Φ) vs Rayleigh number with parameters K and W_2.

it was found that the temperature field became independent of W_2 at large Ra. As expected, Fig. 4 indicates that Φ follows the same trend with respect to W_2. The reason for this behavior is restated concisely as follows. As the thermal boundary layer approaches the heated wall with increasing Ra, cool reservoir fluid finds sufficient access at the outlet to compensate for the inlet configuration. Therefore, the heat transfer rate becomes less dependent on the inflow from the inlet.

Figure 4 also indicates that restrictive W_2 decreases the average non-dimensional heat flux (Φ) at low Ra. This effect is less with an increase in K_r. The reason for this is that with lower values of W_2, less fluid can enter the thermosyphon, so less heat is transferred. However, as is shown in ref. [1], a higher value of K_r tends to increase recirculation at the outlet channel. This is due to the greater thermal buoyancy force imparted to the fluid as K_r is increased and the subsequent decreased thermal boundary layer thickness. The increased recirculation flow compensates for reduced inflow at the inlets due to restrictive W_2, therefore the effect of W_2 on the values of Φ is less at higher values of K_r.

Figure 5 shows large changes in Φ for increased values of K_r. It is evident from the figure that K_r affects Φ more strongly at larger Ra. This is because K_r controls the temperature drop across the heated wall. Convection at the wall surface also plays a role. Larger values of K_r increase the convection coefficient and also decrease the wall temperature drop. Either of these two effects will increase the overall heat transfer. The relative importance of each mechanism is not clear.

So far it is seen that besides Ra, flow restrictions and wall thermal conductivity (represented by W_2 and K_r) are the primary parameters affecting Φ. Let us now consider an optimized case for the present configuration. An 'L' shaped wall resembles the present geometry if the partition wall and right adiabatic wall are removed. In this case flow is not restricted from the top and side, as in the present problem. This minimizes the flow restrictions. If the vertical leg of the 'L' is made isothermal with large thermal conductivity, then the thermal conductivity parameter (K_r) is optimized.

Heat transfer results for this geometry have been published by Rodighiero and de Socio [10]. The authors experimentally examined natural convection near an 'L' shaped body with the vertical side isothermal and the horizontal side adiabatic. The vertical wall material was of high thermal conductivity so that wall conduction was not a parameter. The horizontal side is very long compared with the vertical side. The published experimental heat transfer correlation is given below:

$$Nu_1 = 0.465\, Ra_1^{0.253}. \tag{15}$$

The authors' Nusselt number (Nu_1) and Rayleigh number (Ra_1) above are based on the vertical wall length. Modifications to reflect the Φ and Ra definitions used in the present study are made with the result shown below:

$$\Phi = 0.302\, Ra^{0.253}. \tag{16}$$

This correlation is valid in the laminar range from $Ra = 4630$ to $Ra = 8.3 \times 10^5$. Instability was first observed at the largest Rayleigh number.

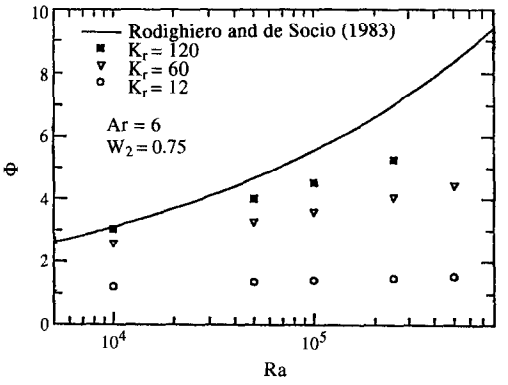

Fig. 6. Published heat transfer results compared with Φ for the present problem.

For comparison purposes, equation (16) is plotted in Fig. 6 along with computed Φ [equation (14)] results of this study. The difference in Φ values at low K_r values clearly shows the effect of low wall conductivity. However, for $K_r = 120$ and in the range up to $Ra = 5 \times 10^4$ the maximum difference in Φ is only 15%. For larger Rayleigh numbers the wall thermal conductivity becomes much more important.

This comparison shows that heat transfer with the present thermosyphon configuration is efficient for sufficiently large K_r and low Ra. As Ra is increased the thermosyphon does not perform as well as the optimized case. Figure 6 indicates that increased K_r will improve the thermosyphon performance. However, increasing K_r yields diminishing results with respect to Φ at large Ra. Recall that Φ is independent of W_2 at large Ra.

It appears that at large Ra, a parameter other than W_2 and K_r becomes important in this comparison. This parameter can only be the presence of the partition and right adiabatic wall. As a result of these, fluid flow is obstructed from approaching the wall. This indicates that while the average non-dimensional heat flux is independent of W_2 at large Ra, other flow restrictions remain. These restrictions include the partition wall and the right vertical wall. Further discussion in this regard can be found in ref. [9].

5. CONCLUSIONS

The heat transfer resulting from an isothermally heated wall-driven flow was investigated for the thermosyphon with two inlets and conducting walls.

The results indicate that the heat transfer becomes independent of the lower inlet configuration as the Rayleigh number is increased ($>2.5\times10^5$). Restrictive lower inlet widths ($W_2 \leqslant 0.25$) strongly reduce the overall heat transfer for Ra less than 10^4.

It is shown in this research that for fixed values of Ra and K_r, the overall heat transfer rate does not change even though the heated wall aspect ratio and thermal conductivity are changed. This observation is in agreement with the findings of ref. [6]. The wall conductivity parameter K_r has important effects. Values of K_r less than 60 severely retard the heat transfer capabilities of the thermosyphon. This is primarily due to conduction resistance at the heated wall and is more pronounced as the Rayleigh number is increased. Conversely, larger values of K_r increase the heat transfer, but this effect gradually decreases as K_r is increased.

Comparison with published experimental results shows that the modified 'U' type thermosyphon examined here is not as effective for heat transfer as the open 'L' wall configuration. However, for K_r of 120 and for relatively low Raleigh numbers (5×10^4), the thermosyphon compares well. This comparison gives the optimized range of values for K_r and Ra for efficient performance of the present thermosyphon configuration. For larger Rayleigh numbers the thermosyphon configuration restricts fluid flow to the heated wall. Thus, less heat transfer occurs relative to the more open 'L' configuration.

REFERENCES

1. J. Fleming and M. Ruhul Amin, Conjugate natural convection in a planar thermosyphon with multiple inlets—I. Velocity and temperature fields, *Int. J. Heat Mass Transfer* **39,** 49–59 (1996).
2. A. E. Zinnes, The coupling of conduction with laminar natural convection from a vertical flat plate with arbitrary surface heating, *J. Heat Transfer* **92,** 528–535 (1970).
3. E. Papanicolaou and Y. Jaluria, Mixed convection from a localized heat source in a cavity with conducting walls: a numerical study, *Numer. Heat Transfer Part A* **23,** 463–484 (1993).
4. D. M. Kim and R. Viskanta, Effect of wall heat conduction on natural convection heat transfer in a square enclosure, *J. Heat Transfer* **107,** 139–146 (1985).
5. G. D. Mallinson, The effects of side-wall conduction on natural convection in a slot, *J. Heat Transfer* **109,** 419–426 (1987).
6. D. A. Kaminski and C. Prakash, Conjugate natural convection in a square enclosure: effect of conduction in one of the vertical walls, *Int. J. Heat Mass Transfer* **29,** 1979–1988 (1986).
7. COSMOS/M Users Manual, Version 1.70, Structural Research and Analysis Corporation, Santa Monica, CA (1993).
8. B. Gebhart, Y. Jaluria, R. L. Mahajan and B. Sammakia, *Buoyancy-induced Flows and Transport*, p. 22. Hemisphere, New York (1988).
9. J. J. Fleming, Conjugate natural convection heat transfer in a planar thermosyphon with multiple inlets, M.S. Thesis, Montana State University, Bozeman, MT (1994).
10. C. Rodighiero and L. M. de Socio, Some aspects of natural convection in a corner, *J. Heat Transfer* **105,** 212–214 (1983).